Applied Catalysis B: Environmental 97 (2010) 213–219

Contents lists available at ScienceDirect

Applied Catalysis B: Environmental

journal homepage: www.elsevier.com/locate/apcatb

Homogeneous photocatalytic mineralization of acetic acid in an aqueous solution of iron ion

Masachiyo Imanishi, Keiji Hashimoto, Hiroshi Kominami*

Department of Applied Chemistry, Faculty of Science and Engineering, Kinki University, 3-4-1 Kowakae, Higashiosaka, Osaka 577-8502, Japan

ARTICLE INFO

Article history:
Received 21 February 2010
Received in revised form 2 April 2010
Accepted 2 April 2010
Available online 10 April 2010

Keywords:
Photocatalyst
Mineralization
Acetic acid
Iron ion

ABSTRACT

Homogeneous photocatalytic mineralization (decomposition to carbon dioxide (CO_2)) of acetic acid in dilute aqueous solutions of various metal ions was examined at room temperature under irradiation of UV light in the presence of oxygen (O_2). Iron ion exhibited a much higher level of activity among the metal ions studied for mineralization of acetic acid. The rate of CO_2 formation was proportional to first-order partial pressure of O_2 and concentrations of iron ion and acetic acid, whereas the rate was in inverse proportional to first-order proton concentration. The rate equation, $r = k\, P_{O_2}\, [[Fe^{III}(H_2O)_6]^{3+}]\, [AcOH]\, [H^+]^{-1}$, in overall photocatalytic mineralization of acetic acid was derived from these results. The mechanism of the photocatalytic mineralization of acetic acid in an aqueous solution of ion was proposed.

1. Introduction

Semiconductor photocatalysts such as titanium(IV) oxide (TiO_2) and tungsten(VI) oxide have been applied to treatment for air pollution and contamination of water as a friendly eco-technology, because air and water containing harmful compounds can be treated without special oxidizing and/or reducing agents using solar light or artificial UV and/or visible light [1–14]. A homogeneous system in which a soluble photocatalyst is used has great potential for photocatalytic treatment of pollutants in water. It is expected that such a homogeneous system has high quantum efficiency since UV light is incident on all of the reagents and photocatalyst. It is hence effective in practical use to apply a homogeneous photocatalyst to the treatment of waste water. However, there have been few studies on treatment for water containing pollutants using a homogeneous system [15–19]. There have been many studies and some reviews and monographs on the mechanism of homogenous photo-oxidation of organic compounds [20–28]. In the literature, the identification of various radicals formed in the elementary reaction steps such as the primary photo-redox step and discrimination of the mode of the primary step were discussed. In the discrimination, three modes of the electron transfer step of Fe^{3+} complex with unidentate ligands were tentatively proposed as the primary photo-physical step: the first is inner-sphere electron transfer involving the photo-oxidation of coordinated ligands by reduction of Fe^{3+} complex to Fe^{2+} complex, the second is outer-sphere electron transfer from an organic solvent molecule to form its organic radical, and the third is outer-sphere electron transfer from an anionic oxidizable ligand to the central atom Fe^{3+} in a dinuclear-bridged complex, forming Fe^{2+} complex and a radical of the ligand molecule or atom. An inner-sphere decomposition was postulated to be the primary photo-redox step for the mechanism of decarboxylation of carboxylic acid over Fe^{3+} complex [18,19,29]. Although it is important in practical use of homogeneous treatments of pollutants in water to reveal the mechanism of the photocatalytic reaction, these mechanisms were not always given by using sufficiently quantitative data and by careful consideration of radical mechanisms for organic reactions. Therefore, the mechanism for homogeneous photocatalytic oxidation of carboxylic acids is still obscure. We therefore kinetically studied the photocatalytic mineralization (decomposition to carbon dioxide (CO_2)) of acetic acid in dilute aqueous solutions of various metal ions under irradiation of UV light in the presence of oxygen (O_2). We briefly reported that iron ion was highly active for homogeneous photocatalytic mineralization of various organic compounds such as acetic acid, alcohols, ketones, phenol and benznesulfonic acid in a dilute solution [30]. In this paper, we present results for (1) the order of activities of various metal ions and (2) the effects of concentrations of acetic acid, iron ion, proton and ligand and partial pressure of O_2 on the activities, and we propose the mechanism of the photocatalytic oxidation of acetic acid in an aqueous solution of iron ion.

* Corresponding author. Tel.: +81 6 6721 2332; fax: +81 6 6727 4301.
E-mail address: hiro@apch.kindai.ac.jp (H. Kominami).

0926-3373/$ – see front matter © 2010 Elsevier B.V. All rights reserved.
doi:10.1016/j.apcatb.2010.04.002

2. Experimental

2.1. Materials

Commercial acetic acid was used without further purification. Metal salts (iron(III) chloride hexahydrate, iron(III) sulfate hydrate, iron(III) bromide, iron(III) nitrate enneahydrate, iron(II) chloride tetrahydrate, copper(II) chloride dihydrate, cobalt(II) chloride hexahydrate, nickel(II) chloride, ruthenium(III) chloride hydrate, manganese(II) chloride tetrahydrate, zinc(II) chloride, chromium(III) chloride hexahydrate, zirconium(IV) chloride, aluminum(III) chloride hexahydrate, silver(I) nitrate, cesium(I) chloride, cerium(III) chloride heptahydrate, lithium(I) chloride, iridium(IV) chloride hydrate, rhodium(III) chloride trihydrate, lanthanum(III) chloride heptahydrate, platinum(IV) chloride, and palladium(II) chloride) were commercial materials of reagent grade and used without further purification.

2.2. Homogeneous photocatalytic mineralization of acetic acid in aqueous solutions

Photo-induced oxidative decomposition of acetic acid was carried out at atmospheric pressure at room temperature in a homogeneous system; a test tube (35 cm^3) of 15 mm in diameter made of Pyrex glass was used as the reactor. A solution (5 cm^3) containing 10 μmol of various metal ions was added to the test tube. After O_2 has been bubbled into the solution for 20 min, the test tube was sealed with a rubber septum. Acetic acid (50 or 200 μmol) was injected into the solution through the rubber septum. The resulting aerated solution was photoirradiated at a wavelength of $\lambda > 300$ nm by a high-pressure mercury arc (400 W, Eiko-sya, Japan) at 298 K. The amount of CO_2 evolved was measured every hour by using a Shimadzu GC-8A gas chromatograph with a Porapack Q column. The amounts of inorganic and organic carbons in the liquid phase were determined by using a Shimadzu TOC Analyzer TOC-Vcs. The activity was defined by initial rate of CO_2 evolution.

2.3. Characterization

UV–vis spectra of iron ion in an aqueous solution of acetic acid were recorded by a Shimadzu UV-2400PC UV–vis spectrophotometer. FTIR spectra of iron ion in acetic acid and deuterium oxide solution of acetic acid were recorded by a Shimadzu FTIR-8300 Infrared Spectrophotometer. The FTIR measurements were carried out by using a liquid mull technique.

3. Results and discussion

3.1. Homogeneous photocatalytic mineralization of acetic acid in dilute aqueous solutions of various ions

Activities of various metal ions were studied at 298 K in homogeneous photocatalytic mineralization of acetic acid in aqueous solutions under irradiation of UV light for 5 h. The results are summarized in Table 1. Heterogeneous photocatalytic mineralization of acetic acid in an aqueous suspension of TiO_2 (Degussa P 25) was also studied under the same conditions for comparison with homogeneous photocatalytic activities of the various ions, and the results are shown in Table 1. The rate of overall photocatalytic mineralization of acetic acid was measured by the formation of CO_2. Iron(III) and iron(II) ions were highly active for photocatalytic mineralization of acetic acid in the homogeneous system. In the photocatalytic mineralization of acetic acid with iron(II) ion, the time course of the concentration of iron(II) ion was studied by complexometry with *o*-phenanthroline using an absorption constant of

Table 1
Rates of CO_2 evolution from acetic acid (200 μmol) in aqueous solutions of metal ions (10 μmol) under O_2 and UV light irradiation.

Metal ion	CO_2 evolution rate/μmol h^{-1}
Fe^{3+}	64
Fe^{2+}	59
Cu^{2+}	2.8
Zr^{4+}	1.7
Cr^{3+}, Mn^{2+}, Co^{2+}, Ni^{2+}, Li^{+}, Cs^{+}, Ag^{+}, Zn^{2+}, Al^{3+}, Ru^{3+}, Rh^{3+}, Ce^{3+}, La^{3+}, Ir^{4+}, Pd^{2+}, Pt^{4+}	<1.0
(TiO_2, P 25, 625 μmol)	70

$\varepsilon_{510} = 1.128 \times 10^4$ dm^3 mol^{-1} cm^{-1} at 510 nm. Though little oxidation of iron(II) ion to iron(III) ion occurred for 30 min in the dark, more than 90% of iron(II) ion was oxidized to iron(III) ion within 30 min under irradiation of UV light. The result supports the idea that the apparent activity observed for iron(II) ion is the same as the activity of iron(III) ion. The activity of iron(III) ion at the concentration of 10 μmol was almost equal to that of TiO_2 (50 mg, 626 μmol). The order of the activities for various metal ions was as follows: $Fe^{3+} \gg Cu^{2+} > Zr^{4+} > Cr^{3+}$, Mn^{2+}, Co^{2+}, Ni^{2+}, Li^{+}, Cs^{+}, Ag^{+}, Zn^{2+}, Al^{3+}, Ru^{3+}, Rh^{3+}, Ce^{3+}, La^{3+}, Ir^{4+}, Pd^{2+}, Pt^{4+}.

3.2. Homogeneous photocatalytic mineralization of acetic acid in aqueous solution of iron(III) ion

Time courses of photocatalytic mineralization of acetic acid in a dilute aqueous solution of iron(III) ion (10 μmol) were studied at 298 K for 5 h under irradiation of UV light, and the results are shown in Fig. 1. Acetic acid (50 μmol) was oxidized to 100 μmol of CO_2 under irradiation of UV light in the presence of iron(III) ion, indicating that stoichiometric and quantitative photocatalytic mineralization of acetic acid to CO_2 occurred as shown in Eq. (1):

$$CH_3COOH + 2O_2 = 2CO_2 + 2H_2O \quad (1)$$

As far as we know, this is the first paper confirming stoichiometry of mineralization of acetic acid in a homogeneous photocatalytic reaction except our previous communication.

Effects of concentration of acetic acid on the reaction rate in the photocatalytic mineralization in an aqueous solution of iron(III)

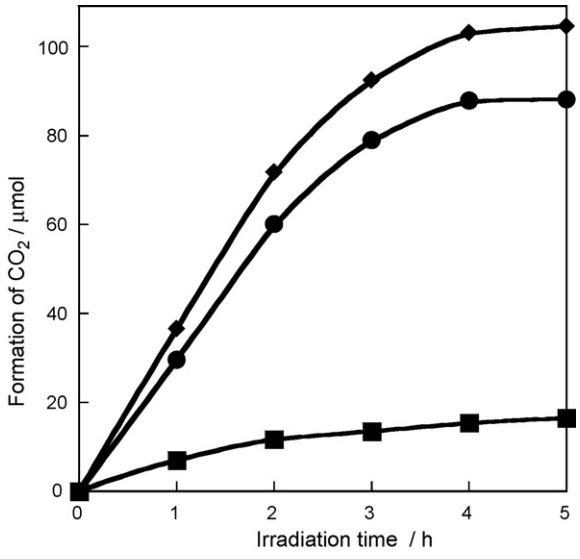

Fig. 1. Time courses of total inorganic carbon (diamonds), CO_2 evolution in gas phase (circles) and inorganic carbon in liquid phase (squares) in the photocatalytic mineralization of acetic acid (50 μmol) in dilute solution of Fe^{3+} (10 μmol) under O_2.

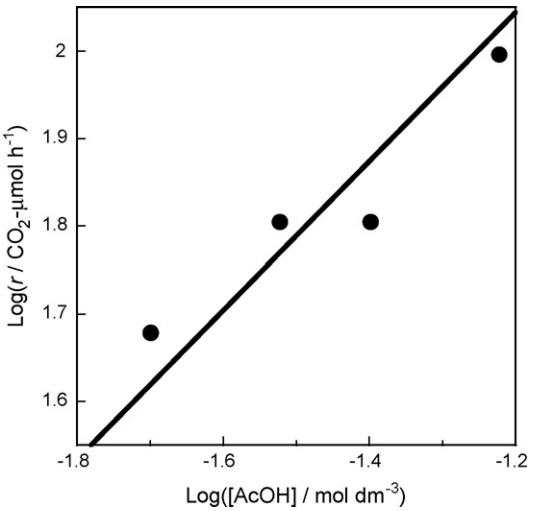

Fig. 2. Effect of concentration of acetic acid (100–300 μmol, corresponding to 0.02–0.06 mol dm^{-3}) on initial rate of photocatalytic mineralization of acetic acid in dilute solution of Fe^{3+} (10 μmol) under O_2.

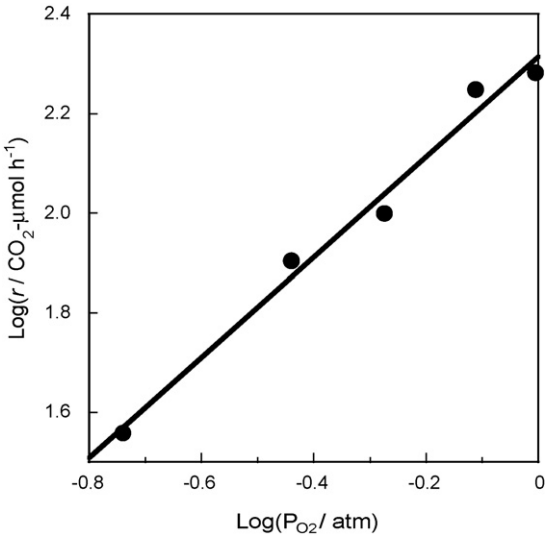

Fig. 4. Effect of partial pressure of O_2 on initial rate of photocatalytic mineralization of acetic acid (200 μmol) in dilute solution of Fe^{3+} (10 μmol) under O_2.

ion (10 μmol) were examined. Fig. 2 shows plots of the logarithm of the initial reaction rate (r) against that of the concentration of acetic acid. A linear relationship was observed between them in the acetic acid concentration range of 0.02–0.06 mol dm^{-3}. The slope of the plots was almost unity, indicating first-order kinetics for the concentration of acetic acid. The first-order dependence proved the presence of an acetic acid ligand in the primary coordination sphere of Fe^{3+} complex. The results suggest that the primary electron transfer step involving absorption of photons by the Fe^{3+} complex coordinated with acetic acid was an outer-sphere electron transfer from the acetic acid ligand to the central atom Fe^{3+} as the primary photo-oxidation step.

Effects of concentration of iron ion on reaction rate in photocatalytic mineralization of acetic acid (200 μmol) in the aqueous solution were examined. Fig. 3 shows plots of the logarithm of r against that of the concentration of iron ion. A linear relationship was observed between them in the iron ion concentration range of 10^{-5} to 10^{-4} mol dm^3. The slope of the plots was almost unity as in the case of plots shown in Fig. 2, indicating first-order kinetics for the concentration of iron ion. The results indicate that Fe^{3+} complex excited by photon absorption was a mononuclear complex in the primary electron transfer step.

Effects of partial pressure of O_2 on reaction rate in photocatalytic mineralization of acetic acid (200 μmol) in an aqueous solution of iron ion (10 μmol) were also investigated. Fig. 4 shows plots of the logarithm of r against that of the partial pressure of O_2. A linear relationship was observed between them in the partial pressure of O_2 range of 0–1.0 atm. The slope of the plots was almost unity, indicating first-order kinetics for the partial pressure of O_2 as well as the concentrations of acetic acid and iron ion.

Effects of proton concentration on reaction rate in photocatalytic mineralization of acetic acid (200 μmol) in an aqueous solution of iron ion (10 μmol) under 1.0 atm of O_2 were studied. Fig. 5 shows plots of the logarithms of r against pH of the solution. A linear relationship was observed between them in the pH range of 1.0–2.2. The logarithm of r was proportional to pH, i.e., inversely proportional to proton concentration, indicating minus first-order kinetics for proton concentration in this pH range. It is known that

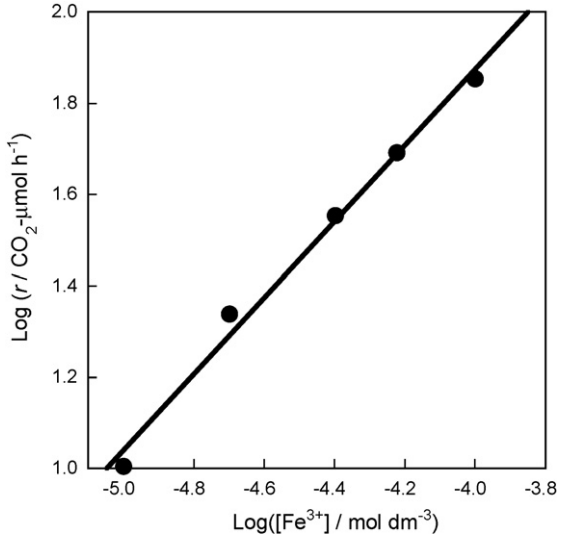

Fig. 3. Effect of concentration of Fe^{3+} (0.05–0.5 μmol, corresponding to 10^{-5} to 10^{-4} mol dm^{-3}) on initial rate of photocatalytic mineralization of acetic acid (200 μmol) in dilute solution of Fe^{3+} under O_2.

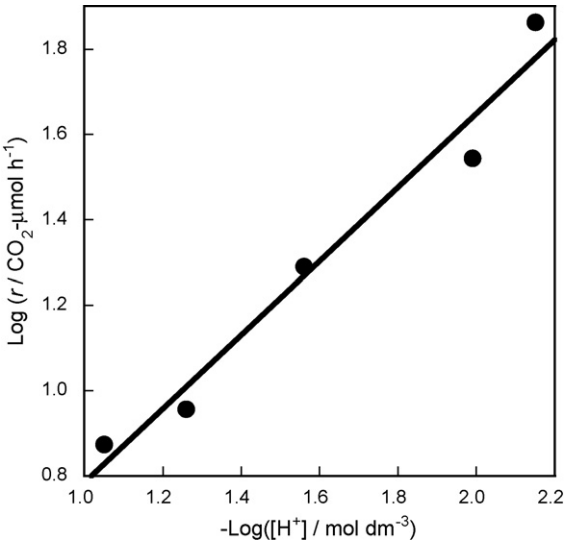

Fig. 5. Effect of concentration of H^+ (pH) on initial rate of photocatalytic mineralization of acetic acid (200 μmol) in dilute solution of Fe^{3+} (10 μmol) under O_2.

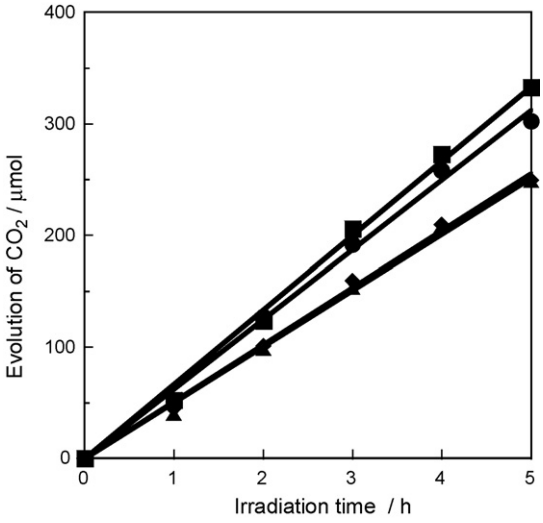

Fig. 6. Time courses of total inorganic carbon in the photocatalytic mineralization of acetic acid (50 μmol) in dilute solutions of iron(III) chloride (circles), nitrate (squares), sulfate (triangles) and bromide (diamonds) (10 μmol, each) on initial rate of photocatalytic mineralization of acetic acid (200 μmol) in dilute solution of Fe^{3+} under O_2.

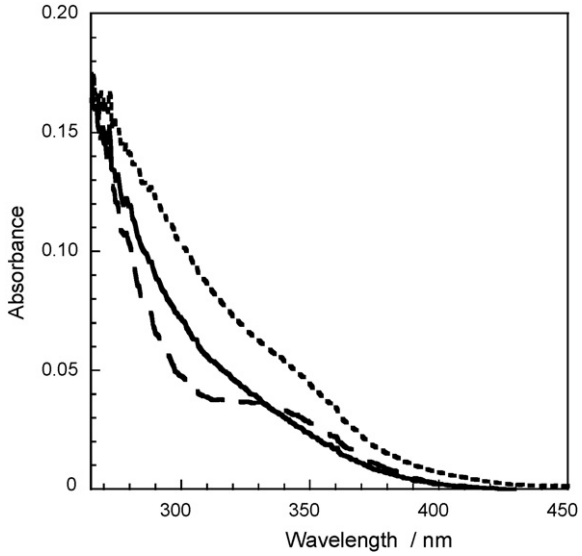

Fig. 7. UV–vis spectra of aqueous solutions of acetic acid (40 mmol dm^{-3}) and iron ion (0.5 mmol dm^{-3}) at pH 2.9 (dotted line), 2.1 (solid line) and 1.5 (broken line).

there are major monomeric Fe^{3+} complex ions of $[Fe^{III}(H_2O)_6]^{3+}$, $[Fe^{III}(OH)\ (H_2O)_5]^{2+}$ and $[Fe^{III}(OH)_2(H_2O)_4]^{+}$ in acidic solution [31–33]; the predominant species is $[Fe^{III}(H_2O)_6]^{3+}$ at pH of less than 2, whereas at pH 2.5–4.0, $[Fe^{III}(OH)(H_2O)_5]^{2+}$ is predominant and $[Fe^{III}(H_2O)_6]^{3+}$ and $[Fe^{III}(OH)_2(H_2O)_4]^{+}$ are minor. At pH 3.0, r was decreased due to the poor solubility of $[Fe^{III}(H_2O)_6]^{3+}$ and no decomposition of CO_2 was observed at pH > 4.3. Although hydroxo complexes, $[Fe^{III}(OH)(H_2O)_5]^{2+}$ and $[Fe^{III}(OH)_2(H_2O)_4]^{+}$, are present in aqueous solution at pH > 4, $[Fe^{III}(H_2O)_6]^{3+}$ is insoluble at pH 4.3. The loss of photocatalytic activity at pH > 4.3 hence excludes the possibility of activities of $[Fe^{III}(OH)(H_2O)_5]^{2+}$ and $[Fe^{III}(OH)_2(H_2O)_5]^{+}$. The result suggests that the photocatalytic mineralization of acetic acid did not involve the formation of $OH^{\bullet}$ radicals, since hydroxo complexes such as $[Fe^{III}(OH)(H_2O)_5]^{2+}$ and $[Fe^{III}(OH)_2(H_2O)_4]^{+}$ are responsible for the generation of $OH^{\bullet}$ radicals under irradiation of UV light [31–35].

Effects of various counter anions (X^-: chloride, bromide, nitrate and sulfate) of iron(III) ions on the photocatalytic reaction rate were studied under the same conditions, and the results are shown in Fig. 6. Little effects of counter anions on the photocatalytic reaction were observed. These results could exclude the possibility of (1) an inner-sphere electron transfer from a coordinated ligand X^- to the central iron atom, forming the radical $X^{\bullet}$ [36,37], (2) an outer-sphere electron transfer from an anion X^- located in the secondary coordination sphere to the exited Fe^{3+} complex [38] and (3) an outer-sphere electron transfer from an anionic oxidizable ligand X^- such as Cl^-, Br^- and NCS^- to the central atom Fe^{3+} within an ion pair [24,36]. The results suggest that the primary photo-redox step involves the photoreduction of Fe^{3+} to Fe^{2+}, accompanied by an inner-sphere electron transfer of the ligand carboxylic group.

A rate equation is experimentally given by using these results:

$$r = k\,P_{O_2}\,[[Fe^{III}(H_2O)_6]^{3+}]\,[AcOH]\,[H^+]^{-1}\,[L]^0, \quad (2)$$

where r, k, P_{O_2}, $[[Fe^{III}(H_2O)_6]^{3+}]$, [AcOH], $[H^+]$ and [L] are initial rate of the photocatalytic reaction, rate constant of overall photo-oxidation, partial pressure of O_2, and concentrations of $[Fe^{III}(H_2O)_6]^{3+}$, acetic acid, proton and ligand, respectively.

3.3. Characterization

Spectra of iron ion in an aqueous solution of acetic acid were recorded over the pH range of 1.5–2.9 at the concentration of 0.5 mmol dm^{-3}. The results are shown in Fig. 7. A band around 330–340 nm appeared. The band agrees with that of dominant species at pH < 2.5, $[Fe^{III}(H_2O)_6]^{3+}$, reported by Langford and Carey [39] and Lam et al. [33]. This species exhibited a maximum absorbance at 240 nm [40]. Likewise, a band at 240 nm was observed in the presence of acetic acid, but the band overlapped with that of acetic acid. Therefore, the band around 330 nm is attributable to $[Fe^{III}(H_2O)_6]^{3+}$. In addition, a band at 400 nm assigned to $[Fe^{III}(OH)(H_2O)_5]^{2+}$ was hardly observed. This result supports the idea that $[Fe^{III}(OH)(H_2O)_5]^{2+}$ is not a dominant species at pH < 2.9.

FTIR spectra of iron(III) chloride in acetic acid and in deuterium oxide solution of acetic acid were measured over the wave number range of 2000–1500 cm^{-1}. The spectra are shown in Fig. 8.

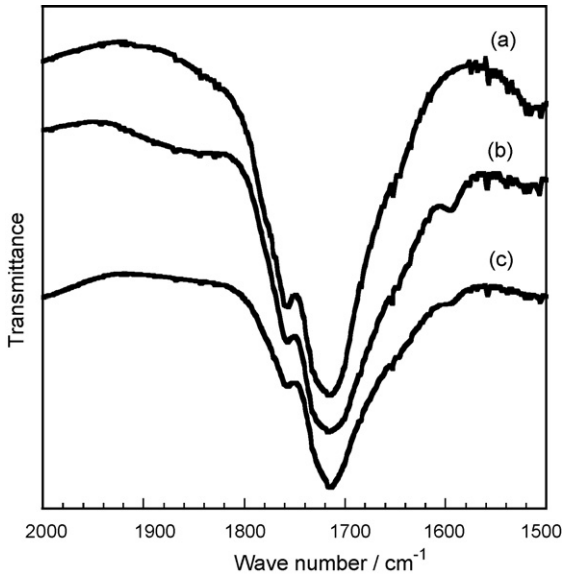

Fig. 8. IR spectra of (a) acetic acid, (b) mixture of acetic acid, deuterium oxide and Fe^{3+}, and (c) the mixture after UV irradiation for 30 min.

The dissolution of iron(III) chloride in the solvents gave a band at 1594 cm^{-1}. Iron(III) chloride hexahydrate had strong bands at 1610 and 1590 cm^{-1} assigned to hydrate coordinated to iron ion. The band at 1594 cm^{-1} is hence attributable to the iron ion coordinated with H_2O. The decrease in strength of the band in deuterium oxide solution can be explained in terms of band shift with an exchange of coordinated H_2O to deuterium oxide. The band also supports the idea that the dominant species at pH < 2.9 is $[Fe^{III}(H_2O)_6]^{3+}$.

3.4. Mechanism of photocatalytic mineralization of acetic acid in aqueous solution of iron(III) ion

It has been reported that there are three modes in the photo-oxidation of carboxylic acids over iron complex ion as the primary photo-redox step [18,19,29]:

$$^{*}[Fe^{III}(RCO_2)]^{2+} \xrightarrow{k_1} Fe^{2+} + R^{\bullet} + CO_2, \quad (3)$$

where $^{*}[Fe^{III}(RCO_2)]^{2+}$ and $R^{\bullet}$ are Fe(III) complex excited by UV light and alkyl radical, respectively. In addition, it is known that radical reaction involves initiation, chain propagation and termination in organic syntheses and that carboxylic acids react with a radical to form CO_2 and a corresponding hydrocarbon radical in autoxidation with O_2 [41]; the O_2 molecule is very facile at combining with free radicals. Moreover, the initiation and/or propagation of acetic acid with $OH^{\bullet}$ radicals generated photochemically from hydroxo iron(III) complexes are probably excluded as described in Fig. 7. In this photocatalytic reaction, the termination due to a reaction between two chain-carrying radicals is negligible, since the concentrations of all radicals formed in initiation and propagation steps are very dilute compared with acetic acid and O_2. Photocatalytic mineralization of acetic acid in an aqueous solution of $[Fe^{III}(H_2O)_6]^{3+}$ probably involves the following reactions:

Equilibrium control

$$[Fe^{III}(H_2O)_6]^{3+} + AcOH \overset{K}{\rightleftarrows} [Fe^{III}(H_2O)_5(AcO)]^{2+} + H_2O + H^{+} \quad (4)$$

Radical initiation reaction (photoreduction of Fe(III) ion)

$$[Fe^{III}(H_2O)_5(AcO)]^{2+} \xrightarrow{k_2} [Fe^{II}(H_2O)_5]^{2+} + AcO^{\bullet} \quad (5)$$

Chain propagation

$$AcO^{\bullet} \xrightarrow{k_3} {}^{\bullet}CH_3 + CO_2 \quad (6)$$

$$^{\bullet}CH_3 + O_2 \xrightarrow{k_4} CH_3OO^{\bullet} \quad (7)$$

$$CH_3OO^{\bullet} + AcOH \xrightarrow{k_5} CH_3OOH + AcO^{\bullet} \quad (8)$$

$$CH_3O^{\bullet} + O_2 \xrightarrow{k_6} H_2O + CO_2 + H^{\bullet} \quad (9)$$

Self-decomposition

$$CH_3OO^{\bullet} \xrightarrow{k_7} CH_3O^{\bullet} + (1/2)O_2 \quad (10)$$

Decomposition of methyl hydroperoxide

$$CH_3OOH + [Fe^{II}(H_2O)_5]^{2+} \xrightarrow{k_8} CH_3O^{\bullet} + OH^{-} + [Fe^{III}(H_2O)_5]^{3+} \quad (11)$$

Termination

$$2H^{\bullet} + (1/2)O_2 \rightarrow H_2O \quad (12)$$

Neutralization

$$OH^{-} + H^{+} \rightarrow H_2O \quad (13)$$

Coordination

$$[Fe^{III}(H_2O)_5]^{3+} + H_2O \rightleftarrows [Fe^{III}(H_2O)_6]^{3+} \quad (14)$$

The reaction rates in Eqs. (12)–(14) are assumed to be very fast compared with those in the other steps. Since an equilibrium is attained in Eq. (4), the product of K, $[[Fe^{III}(H_2O)_6]^{3+}]$ and [AcOH] is equal to that of $[H^{+}]$, $[H_2O]$ and $[[Fe^{III}(H_2O)_5(AcO)]^{2+}]$, where K, $[[Fe^{III}(H_2O)_6]^{3+}]$, [AcOH], $[H^{+}]$, $[H_2O]$, and $[[Fe^{III}(H_2O)_5(AcO)]^{2+}]$ are equilibrium constant and concentrations of $[Fe^{III}(H_2O)_6]^{3+}$, acetic acid, proton, water and $[Fe^{III}(H_2O)_5(AcO)]^{2+}$ complex, respectively. The concentration of $[Fe^{III}(H_2O)_5(AcO)]^{2+}$ is defined as follows:

$$[[Fe^{III}(H_2O)_5(AcO)]^{2+}] = \frac{K[[Fe^{III}(H_2O)_6]^{3+}][AcOH]}{[H^{+}][H_2O]}. \quad (15)$$

From the steady-state treatment, the rate of formation of $[Fe^{II}(H_2O)_5]^{2+}$ in Eq. (5) is equal to the rate of its disappearance in Eq. (11):

$$I\phi k_2[[Fe^{III}(H_2O)_5(AcO)]^{2+}] = k_8[CH_3OOH][[Fe^{II}(H_2O)_5]^{2+}], \quad (16)$$

where I, ϕ, k_2, k_8, $[CH_3OOH]$ and $[[Fe^{II}(H_2O)_5]^{2+}]$ are photon flux, absorption efficiency, rate constant for radical initiation in Eq. (5), rate constant for decomposition of methyl hydroperoxide (CH_3OOH) with $[Fe^{II}(H_2O)_5]^{2+}$ in Eq. (11), concentration of CH_3OOH and concentration of $[Fe^{II}(H_2O)_5]^{2+}$, respectively. The value for $[CH_3OOH]$ from Eq. (16) may be substituted into Eq. (15) to give

$$[CH_3OOH] = \frac{I\phi K k_2[[Fe^{III}(H_2O)_6]^{3+}][AcOH]}{k_8[[Fe^{II}(H_2O)_5]^{2+}][H^{+}][H_2O]}. \quad (17)$$

From the steady-state treatment, the rate of disappearance of acetyl radical ($AcO^{\bullet}$) in Eq. (6) is equal to the sum of the rates of its formation in Eqs. (5) and (8):

$$k_3[AcO^{\bullet}] = \frac{I\phi K k_2[[Fe^{III}(H_2O)_6]^{3+}][AcOH]}{[H^{+}][H_2O]} + k_5[CH_3OO^{\bullet}][AcOH], \quad (18)$$

where k_3, k_5 and $[CH_3OO^{\bullet}]$ are rate constant for formation of methyl radical in Eq. (6), rate constant for its disappearance of methyl peroxide radical ($CH_3OO^{\bullet}$) in Eq. (8) and concentration of $CH_3OO^{\bullet}$, respectively. From the steady-state treatment, the rate of formation of the $^{\bullet}CH_3$ in Eq. (6) is equal to the rate of its disappearance in Eq. (7):

$$k_4 P_{O_2}[^{\bullet}CH_3] = k_3[AcO^{\bullet}]. \quad (18')$$

where k_4, P_{O_2} and $[^{\bullet}CH_3]$ are rate constant for disappearance of $^{\bullet}CH_3$ in Eq. (7), partial pressure of O_2 and concentration of $^{\bullet}CH_3$, respectively. From the steady-state treatment, the rate of disappearance of the methoxyl radical ($CH_3O^{\bullet}$) in Eq. (9) is equal to the sum of the rates of its formation:

$$k_6 P_{O_2}[CH_3O^{\bullet}] = \frac{I\phi K k_2[[Fe^{III}(H_2O)_6]^{3+}][AcOH]}{[H^{+}][H_2O]} + k_7[CH_3OO^{\bullet}], \quad (19)$$

where k_6, k_7 and $[CH_3O^{\bullet}]$ are rate constant for disappearance of $CH_3O^{\bullet}$ in Eq. (9), rate constant for decomposition of $CH_3OO^{\bullet}$ in Eq. (10) and concentration of $CH_3O^{\bullet}$, respectively. From the steady-state treatment, the rate of formation of the $CH_3OO^{\bullet}$ in Eq. (7) is equal to the sum of the rates of its disappearance in Eqs. (8) and (10):

$$k_4 P_{O_2}[^{\bullet}CH_3] = k_5[CH_3OO^{\bullet}][AcOH] + k_7[CH_3OO^{\bullet}] = [CH_3OO^{\bullet}](k_5[AcOH] + k_7). \quad (20)$$

One might consider changing the concentrations of $AcO^{\bullet}$, $CH_3OO^{\bullet}$, $^{\bullet}CH_3$ and $CH_3O^{\bullet}$ in belief that there would be no change in their rate constants if the photo-oxidation rapidly attains a steady state in the initial reaction period. In addition, the terms of the concentration of acetic acid and partial pressure of O_2 are

considered to be constant, since acetic acid and O_2 in the initial reaction are in large excess under a constant pressure, compared with $[Fe^{III}(H_2O)_6]^{3+}$ and radicals. The concentrations of $AcO^{\bullet}$, $CH_3OO^{\bullet}$, $^{\bullet}CH_3$ and $CH_3O^{\bullet}$ are defined as x, y, z and q, respectively. Therefore, Eqs. (18), (18′), (19) and (20) are a system of linear equations with four unknowns. Solving their simultaneous equations, x, y, z and q are calculated to be

$$x = \frac{I\phi K k_2[[Fe^{III}(H_2O)_6]^{3+}][AcOH](1 + k_5[AcOH]/k_7)}{k_3[H^+][H_2O]},$$

$$y = \frac{I\phi K k_2[[Fe^{III}(H_2O)_6]^{3+}][AcOH]}{k_7[H^+][H_2O]},$$

$$z = \frac{I\phi K k_2[[Fe^{III}(H_2O)_6]^{3+}][AcOH](1 + k_5[AcOH]/k_7)}{k_4 P_{O_2}[H^+][H_2O]}, \text{ and}$$

$$q = \frac{2I\phi K k_2[[Fe^{III}(H_2O)_6]^{3+}][AcOH]}{k_6 P_{O_2}[H^+][H_2O]}.$$

The rate of the overall photo-oxidation, r, is equal to formation rate of CO_2 in Eqs. (6) and (9):

$$r = \frac{d[CO_2]}{dt} = k_3[AcO^{\bullet}] + k_6 P_{O_2}[CH_3O^{\bullet}]. \quad (21)$$

The solutions of $[AcO^{\bullet}]$ and $[CH_3O^{\bullet}]$ from x and q may be substituted into Eq. (21) to give

$$\frac{d[CO_2]}{dt} = \frac{I\phi K k_2[[Fe^{III}(H_2O)_6]^{3+}][AcOH](3 + k_5[AcOH]/k_7)}{[H^+][H_2O]}. \quad (22)$$

If $k_7 \gg k_5$,

$$\frac{d[CO_2]}{dt} \approx \frac{3I\phi K k_2[[Fe^{III}(H_2O)_6]^{3+}][AcOH]}{[H^+][H_2O]}. \quad (23)$$

In agreement with Eq. (23), the experimental photo-oxidation rate in Eq. (2) has been shown to be proportional to the concentration of Fe(III) ion and that of acetic acid and reversely proportional to the concentration of proton. The solutions were calculated with the assumption that the term of partial pressure of O_2 is a constant because of the large excess of O_2. However, the reaction equation is described under a variation of O_2 pressure as follows. Eq. (24) is given by substituting $k_4\,[^{\bullet}CH_3]\,P_{O_2}$ for $k_3\,[AcO^{\bullet}]$ in Eq. (23):

$$\frac{d[CO_2]}{dt} = k_4 P_{O_2}[^{\bullet}CH_3] + k_6 P_{O_2}[CH_3O^{\bullet}]$$
$$= P_{O_2}\{k_4[^{\bullet}CH_3] + k_6[CH_3O^{\bullet}]\}. \quad (24)$$

Since the term of the partial pressure of O_2, P_{O_2}, is proportional to the pressure of O_2, P_{O_2}, Eq. (24) indicates that the rate of overall photo-oxidation depends on the partial pressure of O_2 in first order.

4. Conclusions

Acetic acid (50 μmol) was quantitatively oxidized to form 100 μmol of CO_2 under irradiation of UV light in the presence of Fe(III) ion. The activity of iron(III) ion at the concentration of 10 μmol was almost equal to that of TiO_2 (50 mg, 626 μmol). The order of the activities for various metal ions is as follows: $Fe^{2+} \approx Fe^{3+} \gg Cu^{2+} > Zr^{4+} > Cr^{3+}$, Mn^{2+}, Co^{2+}, Ni^{2+}, Li^{+}, Cs^{+}, Ag^{+}, Zn^{2+}, Al^{3+}, Ru^{3+}, Rh^{3+}, Ce^{3+}, La^{3+}, Ir^{4+}, Pd^{2+}, Pt^{2+}.

The effects of concentrations of acetic acid and Fe(III) ion and partial pressure of O_2 on the photo-oxidation rate of acetic acid gave, respectively, a good first-order plot in the concentrations of acetic acid and Fe(III) ion and partial pressure of O_2. However, the rate dependence on the concentration of proton gave a good minus first-order plot in proton concentration over the pH range of 1–4.0. The photocatalytic activity disappeared at pH of 4.3 because $[Fe^{III}(H_2O)_6]^{3+}$ was insoluble in water at pH of 4.3. These results experimentally gave the following rate equation:

$$r = k\,P_{O_2}\,[[Fe^{III}(H_2O)_6]^{3+}]\,[AcOH]\,[H^+]^{-1}.$$

We proposed the mechanism of photocatalytic mineralization of acetic acid, in which the rate-controlling step is photocatalytic reduction of Fe(III)–acetate complex ion to Fe(II) complex ion. The rate equation is given from the mechanism under a constant pressure of O_2 as follows:

$$\frac{d[CO_2]}{dt} \approx \frac{3I\phi K k_2[[Fe^{III}(H_2O)_6]^{3+}][AcOH]}{[H^+][H_2O]}$$

The rate equation is given from the mechanism under changing pressure of O_2 as follows:

$$\frac{d[CO_2]}{dt} = P_{O_2}\{k_4[^{\bullet}CH_3] + k_6[CH_3O^{\bullet}]\}.$$

Therefore, the experimental results can be explained well by the proposed mechanism.

References

[1] M.A. Fox, M.T. Dulay, Chem. Rev. 93 (1993) 341.
[2] M.R. Hoffmann, S.T. Martin, W. Choi, D.W. Bahnemann, Chem. Rev. 95 (1995) 69.
[3] R. Asahi, T. Morikawa, T. Ohwaki, K. Aoki, Y. Taga, Science 293 (2001) 269.
[4] T. Ohno, M. Akiyoshi, T. Umebayashi, K. Asai, T. Mitui, M. Matsumura, Appl. Catal. A 265 (2004) 115.
[5] H. Irie, S. Miura, K. Kamiya, K. Hashimoto, Chem. Phys. Lett. 457 (2008) 202.
[6] R. Abe, H. Takami, N. Murakami, B. Ohtani, J. Am. Chem. Soc. 130 (2008) 7780.
[7] T. Arai, M. Horiguchi, M. Yanagida, T. Gunji, H. Sugihara, K. Sayama, Chem. Commun. (2008) 5565.
[8] H. Yamashita, H. Nose, Y. Kuwahara, Y. Nishida, S. Yuan, K. Mori, Appl. Catal. A 350 (2008) 164.
[9] M. Kitano, M. Matsuoka, M. Ueshima, M. Anpo, Appl. Catal. A 325 (2007) 1.
[10] H. Yamashita, Y. Ichihashi, S.-G. Zhang, Y. Matsumura, Y. Souma, T. Tatsumi, M. Anpo, Appl. Surf. Sci. 121 (1997) 305.
[11] H. Kominami, K. Takenouchi, K. Hashimoto, K. Sayama, Electrochemistry 76 (2007) 118.
[12] K. Maeda, T. Takata, M. Hara, N. Saito, Y. Inoue, H. Kobayashi, K. Domen, J. Am. Chem. Soc. 127 (2005) 8286.
[13] K. Hashimoto, M. Osaki, E. Shono, K. Adachi, H. Kominami, Y. Kera, Appl. Catal. B 30 (2001) 429.
[14] K. Hashimoto, K. Sumida, S. Kitano, K. Yamamoto, N. Kondo, Y. Kera, H. Kominami, Catal. Today 144 (2009) 37.
[15] S. Adrianirinaharivelo, J.F. Pilichowski, M. Bolte, Transit. Met. Chem. 18 (1993) 37.
[16] J.J. Pignatello, Y. Sun, ACS Symp. Ser. (1993) 77.
[17] H. Parlar, in: D.H. Hutson, T.R. Roberts (Eds.), Environmental Fate of Pesticides, Wiley, New York, 1990, pp. 245.
[18] P. Maruthamuthu, R.E. Huie, Chemosphere 30 (1995) 2199.
[19] L. Vincze, S. Papp, J. Photochem. 36 (1987) 279.
[20] J. Šima, J. Makáňová, Coord. Chem. Rev. 160 (1997) 161.
[21] T.D. Waite, Handbook of Enviromental Chemistry, vol. 2, 2005, p. 255.
[22] K. Kalyanasundaram, Photochemistry of Polypyridine and Porphyrin Complexes, Academic Press, New York, 1992.
[23] J. Šima, in: J.W. Buchler (Ed.), Complexes with Tetrapyrrole Ligands III, Structure Bonding, vol. 84, 1995, p. 135.
[24] O. Horváth, K.L. Stevenson, Charge Transfer Photochemistry of Coordination Compounds, Verlag Chemie, New York, 1993, p. 207.
[25] H. Hennig, D. Rehorek, Photochemische und Photokatalytische Reaktionen von Koordinationsverbindungen, Acad. Verlag, Berlin, 1987.
[26] H. Hennig, L. Weber, D. Rehorek, Adv. Chem. Ser. 238 (1993) 351.
[27] R.G. Solomon, S. Ghosh, S. Raychaudhuri, Adv. Chem. Ser. 238 (1993) 315.
[28] H. Ohtaki, T. Radnai, Chem. Rev. 93 (1993) 1157.
[29] M. Bideau, L. Faure, Y. Assemian, B. Claudel, J. Mol. Catal. 43 (1988) 267.
[30] M. Imanishi, K. Hashimoto, H. Kominami, Chem. Lett. in press.
[31] W. Feng, D. Nansheng, Chemosphere 41 (2000) 1137.
[32] L. Lopes, J. de Laat, B. Legude, Inorg. Chem. 41 (2002) 2505.
[33] S.W. Lam, K. Chiang, T.M. Lim, R. Amal, G.K.-C. Low, J. Catal. 234 (2005) 292.
[34] H. Krysova, J. Jirkovsky, J. Krysa, G. Mailhot, M. Bolte, Appl. Catal. B 40 (2003) 1.
[35] H. Mest'akova, G. Mailhot, J. Jirkovsky, J. Krysa, M. Bolte, Appl. Catal. B 57 (2005) 257.
[36] V. Balzani, V. Carassiti, Photochemistry of Coordination Compounds, Academic Press, New York, 1970.

[37] A.I. Kryukov, S.J. Kutschmij, Fotochimiya Kompleksov Perechodnych Metallov, Naukova Dumka, Kiev, 1989, p. 128.
[38] I.V. Khmelnickij, K.A. Amosov, V.F. Pliusnin, V.P. Grivin, Koord. Khim. 16 (1990) 1373.
[39] C.H. Langfold, J.H. Carey, Can. J. Chem. 53 (1975) 2430.
[40] B.C. Faust, J. Hoigne, Atmos. Environ. 24A (1990) 79.
[41] J. Hine, Physical Organic Chemistry, Second ed., McGraw-Hill Book Company, Inc., 1962, pp. 402–483.